Spectral Characterization of Rank Filters Based Directional Textures of Digital Images Using Rajan Transform

Naveed Farhana and Nisar Hundewale

College of Computers and Information Technology, Taif University,
Taif, Kingdom of Saudi Arabia
{n.farhana,n.hundewale}@tu.edu.sa

Abstract. Tissue characterization with the help of ultrasound images has remained an unsolvable problem to clinicians till date. Many techniques have been suggested to solve this issue. Yet a complete solution has not been arrived at so far. This paper gives a new technique which would indeed lead to the formulation of a robust method for characterizing tissues from ultrasound images. Any given image is processed using what we call as rank filters which would detect textures in four different directions. Various spatial features of these textures such as corners, curves, dots and lines are detected independently using the spectral domain pattern recognizing capabilities of Rajan Transform, which is a homomorphic transform developed on the lines of Hadamard Transform. The histogram analysis of these features would finally lead to spectral characterization of tissue textures. Clinicians would be able to resolve then the problem of tissue characterization.

Keywords: Ultrasound, Texture analysis, Rank Filter, Rajan Transform.

1 Introduction

Ultrasound imaging [1],[2],[3] can be performed by emitting a pulse, which is partially reflected from a boundary between two tissue structures, and partly transmitted. The reflection depends on the , difference between the impedance of the two tissues. Basic imaging by ultrasound does merely use the amplitude information in the reflected signal. One pulse is emitted, the reflected signal, however, is sampled somewhat continuously. As the velocity of sound in tissue is almost invariant, the time between the emission of a pulse and the reception of a reflected signal is dependent on the distance; that is, the depth of the reflecting structure. Different structures will reflect with different amount of the emitted energy. Thus the reflected signal from different depths will have variant amplitudes. The time before a new pulse is sent out depends on the maximum desired depth that is desired to image. This works more or less on the principles of a radar. Also, the apparent density of the tissue on the ultrasound image depends on the fiber direction. For example, a part of the heart where the fibers run mainly in a direction across the ultrasound beams will

N. Meghanathan et al. (Eds.): CCSIT 2012, Part III, LNICST 86, pp. 225–238, 2012.

appear much denser. Variations in amplitude do not necessarily mean differences in density, but may also mean variations in reflectivity due to variation in the incident and reflected angles. Thus, integrated backscattering can be used for analysis of cyclicity, but it is not much useful for tissue characterization.

Tissue characterization [4], [5] ,[6]could be carried out using texture analysis[5][6] of the tissues from the acquired image. Spectral characterization [7],[8],[9],[10] of the textures would finally lead to tissue characterization. This paper introduces a novel technique of 'Spectral Characterization of Rank Filters Based Directional Textures of Ultrasound Images[11],[12] ,[13] Using Rajan Transform[14].

Let us briefly review the basics of Rajan Transform and then proceed to study as to how to use this transform for pattern recognition.

1.1 Rajan Transform

Rajan Transform (RT) is a fast transform which is a variant of **Hadamard Transform** (HT) structurally similar to the Decimation-In-Frequency Fast Fourier Transform algorithm. RT is applicable to any arbitrary number sequence of length of power of 2. The two basic operations involved in this fast transform are (i) addition and (ii) difference. Given a number sequence x(n) of length a power of 2, first it is divided into the first half and the second half each consisting of (N/2) points so that the following hold good.

$$g(i) = x(i) + x(i + (N / 2)); 0 \le j \le N/2 ; 0 \le i \le N/2$$

$$h(i) = |x(i) - x(i - (N / 2))|; 0 \le j \le N/2 ; N/2 \le i \le N$$

Now each (N/2)–point segment is further divided into two halves each consisting of (N/4) points so that the following hold good.

$$g1(k) = g(j) + g(j + (N / 4)); 0 \le k \le N/4 ; 0 \le j \le N/4$$

$$g2(k) = |g(j) - g(j - (N/4))|; 0 \le k \le N/4 ; N/4 \le j \le N/2$$

$$h1(k) = h(j) + h(j + (N/4));0 \le k \le N/4; 0 \le j \le N/4$$

$$h2(k) = |h(j) - h(j - (N/4))|;0 \le k \le N/4 ; N/4 \le j \le N/2$$

This process is continued till no more division is possible. The total number of stages thus turns out to be $\log_2 N$ .Let us denote the sum and difference operators respectively as + and ~. If x(n) is a number sequence of length $N = 2^k$; K>0, then its Rajan Transform is denoted as X(k). X (k) is also called 'Rajan Spectrum'. The signal flow graph of RT for an 8-point sequence is shown below.

The forward transform can be obtained by operating the input sequence using a matrix called R matrix, recursively by dividing input sequence as well as by partitioning the R matrix in the following manner.

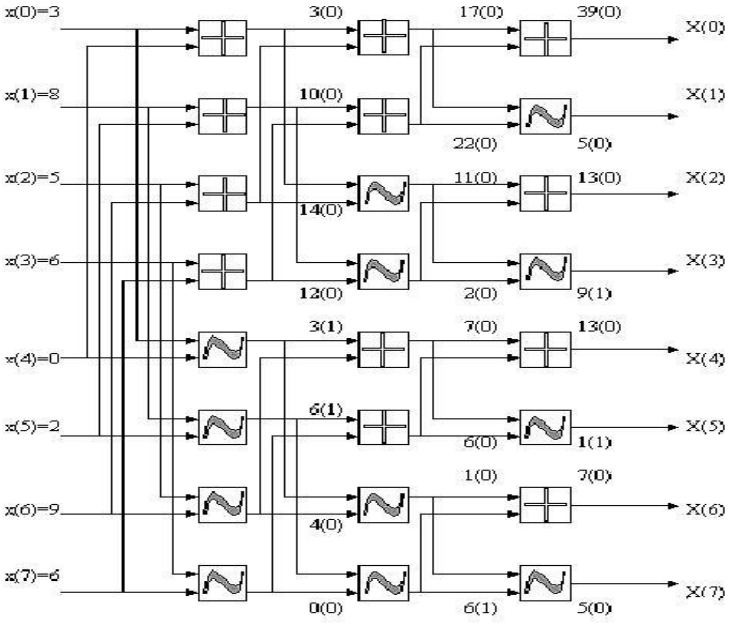

Fig. 1. Signal flow diagram of RT for a 8- point sequence

$$A_{N\times 1} = R_N \times X_{N\times 1}$$

$$\text{where } R_N = \begin{bmatrix} I_{N/2} & I_{N/2} \\ -e_k I_{N/2} & e_k I_{N/2} \end{bmatrix} \text{ of size } N \times N$$

X is the column matrix having input sequence of length N. $I_{N/2}$ is the identity matrix of size N/2, that is, half the size of the input sequence matrix $X_{Nx1.}$ Basic identity matrix $I_1 = 1$; and e_k is the encryption function with k as encryption value which is defined as.

$e_k = (-1)^K$ Such that

k = 1; for x(i+N/2)≤x(i); 0≤i≤N/2.

k = 0; otherwise.

And x(i) is the i^{th} element of matrix $X_{Nx1.}$ Now divide the matrix X_{Nx1} into two column matrices, namely. A_{00} and A_{01} of size N/2 and treating these matrices as two input sequences, compute the two new A_{10} and A_{11} matrices by using the operator $R_{N/2}$ for both sequences. Note the size of the R matrices used is one half of the original R_N matrix. Continue the above procedure iteratively till the size of the sub matrices is reduced to two. So, we have $N=2^{n-p}$, for p^{th} iteration stage, p=1,2,…,n. All the encryption binary values, that k values thus generated during the process of

computation per iteration are to be associated with the final spectrum, to recover the original sequence through inverse transformation technique. Note that this closed form expression precisely defines the algorithms stated in the beginning of this section.

1.2 Inverse Rajan Transform

Now, in order to work with sequences containing negative sample values, we proceed as usual in the case of forward transform. But, the inverse transform is calculated just by adding a constant value $N(2^M-1)$ to the CPI value of the spectrum. M is the bit length required to represent the maximum quantization level of the samples and N is the length of the sequence. This constant factor $k=(2^M-1)$ is chosen such that all the maximum possible negative values of the sequence x(n) are level shifted to 0 or above. This DC shift is required, because we hide the sign of the negative values that are generated while computing the forward RT. As mentioned earlier, RT induces an isomorphism between the domain set consisting of the Inverse, Cyclic, Dyadic and Dual class permutations of a sequence on to a range set consisting of sequences of the form X(k)E(r) where X(k) denotes the permutation invariant RT and E(r) an encryption code corresponding to an element in the domain set. This map is a one-to-one and on-to correspondence and an inverse map also exists. Thus RT is viewed as a transform. Now we provide a technique for obtaining the inverse of Rajan Transform.

Inverse Rajan Transform is a recursive algorithm and it transforms a RT code X(k)E(r) of length N(1+m) where $N=2^m$ and m is the number of stages of computation, into one of its original sequences belonging to its permutation class depending on the encryption code E(r). The computation of IRT is carried out in the following manner. First the input sequence is divided into segments each consisting of two points so that either

$$g(2j+1) = (X(2k) + X(2k+1))/2$$

$$g(2j) = \max(X(2k), X(2k+1)) - g(2j+1)$$

$$\text{if } E_1(2r)=0 \text{ and } E_1(2r+1) = 0;\ 0\le j\le N;\ 0\le k\le N;\ 0\le r\le N$$

or

$$g(2j) = (X(2k) + X(2k+1))/2$$

$$g(2j+1) = \max(X(2k), X(2k+1)-g(2j)$$

$$\text{if } E_1(2r) = 1 \text{ or } E_1(2r+1) = 1; \quad 0\le j\le N;\ 0\le k\le N;\ 0\le r\le N$$

The resulting sequence is divided into segments each consisting of four points. Each 4-point segment is synthesized as per the above procedure. The resulting sequence is further divided into segments each consisting of eight points and the same procedure is carried out. This process is continued till no more division is possible.

Consider X(k)=39,5,13,9,13,1,7,5. The inverse x(n) is obtained from the given X(k)E(r) as shown is Fig 3.2.1.1 The symbols '^', '>' and '~' respectively denote the operators average of two, maximum of two and difference of two. Note that IRT will work only in the presence of encryption sequence E(r) and for every member of the permutation class there would be a unique encryption sequence. Study of the class of encryption sequences corresponding input sequences itself is a field of active research. As already out lined that RT hides negative signs and so it is important to add $N(2^M-1)$ to X(0) in order to get back the original sequence.

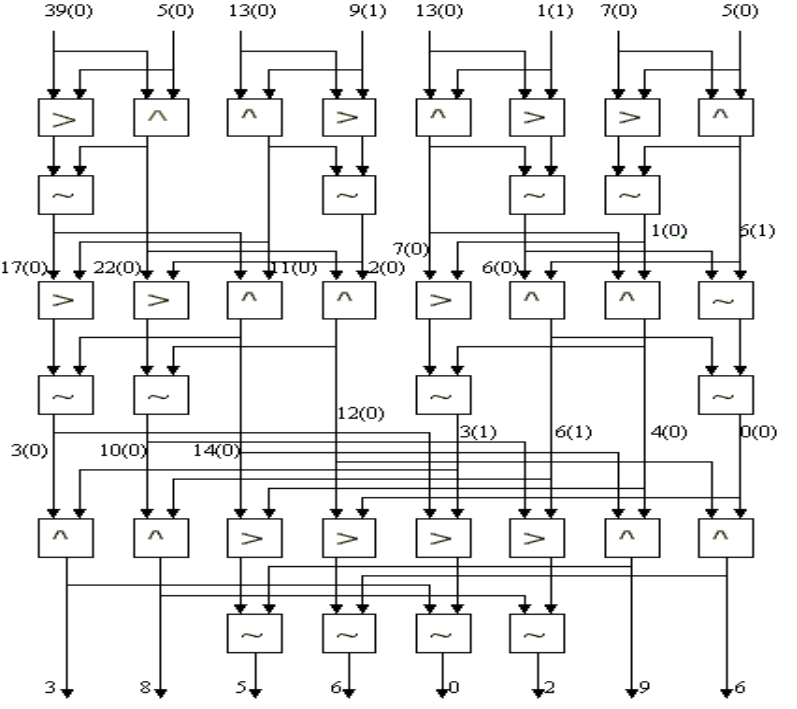

Fig. 2. Signal flow diagram of IRT of a spectral sequence

Let X_{Nx1} be the column matrix of the RT coefficients of length N, and the associated encryption values generated per iteration are orderly arranged in the form of column matrices $E^1, E^2, \ldots, E^{n+1}$, of length N/2, Where $n=\log_2 N$. For N=8, we have E^1 and E^2, two encryption matrices of size 4X1 with binary encryption values as elements. Here X_{NX1} is the RT coefficient matrix. R_{NX1} is the intermediate matrix. $A_{Nx1}$is matrix with the elements positioned in their appropriate positions using the encryption matrix E^r corresponding to the current iteration. E^r is the matrix obtained by element wise

complementing the E^r matrix, where r=n-1,n-2,….,1. Since we trace back the forward algorithm, we start initially with $N=2^p$, where p=1, 2, 3,…,n. Hence, we use initially the encryption matrix that is generated at the last stage of forward RT computation and further use the remaining matrices in the reverse order for IRT computation. Each encryption matrix is to be partitioned as per the requirement.

$$[R_{N\times 1}] = \begin{bmatrix} \max(x_1, x_{1+N/2}) \\ \vdots \\ \max(x_{N/2}, x_N) \\ 0 \\ \vdots \\ \text{upto } \frac{N}{2} \text{ (zeros)} \end{bmatrix} - \frac{1}{2}\begin{bmatrix} I_{N/2} & I_{N/2} \\ -I_{N/2} & -I_{N/2} \end{bmatrix} [X_{N\times 1}]$$

$$[A_{N\times 1}] = \begin{bmatrix} I_{N/2} & I_{N/2} \\ I_{N/2} & I_{N/2} \end{bmatrix} [R_{N\times 1}] - \begin{bmatrix} [E^r_{N/2}][I_{N/2}] & \overline{[E^r_{N/2}]}_{L\text{-}N/2} \\ \overline{[E^r_{N/2}]}[I_{N/2}] & [E^r_{N/2}][I_{N/2}] \end{bmatrix} [R_{N\times 1}]$$

The closed form expression shown as equation above represents the Inverse Rajan Transform. For example, let us consider a sequence x(n) which has a maximum sample value of 15. The RT of this sequence is X(k). No one can assume the value of M to be 4 so that the maximum negative sample value in sequence is -15. Addition of +15 to each sample value in a 8-point input sequence x(n) will lead to the sequence,

$$x_1(k)=x(0)+15,x(1)+15, \ldots,x(7)+15$$

Which is level shifted to 0 and above. Now the spectrum of this level shifted sequence $x_1(n)$ would be

$$X_1(k)=X_1(0),X_1(1), \ldots,X_1(7),$$

$$\text{where } X_1(0) = X(0)+120, X_1(1)=X(1), \ldots,X_1(7) = X(7).$$

One can use RT for developing various pattern recognition algorithms like (i) corner detection, (ii) curves detection, (iii) dots detection and (iv) lines detection [15],[16]. In addition, algorithms for classifying textures and for computing volume fraction are also provided in the sequel with suitable example images.

2 RT Based Pattern Recognition Algorithms

2.1 Corners Detection

Please On every move of the 3X3 window, the RT spectral sequence, say, X(0), X(1), X(2), X(3), X(4), X(5), X(6), and X(7) corresponding to the sequence of the numbered cell values is checked for the following:

(i) Corners due to pairs of lines subtending an angle of 45° or its integral multiples:

1. The number of RT elements that are less than T must be 4.
2. RT elements X[0], X[2], X[4], X[6] must be greater than T.

(ii) Corners due to pairs of lines subtending 90° or its integral multiples:

1) The number of RT elements that are less than T must be 4.
2) RT elements X[0], X[1], X[4],X[5] must be greater than T.

The above procedure is repeated till the entire image is scanned. The overall effect is that the resulting image would consist only of corner points.

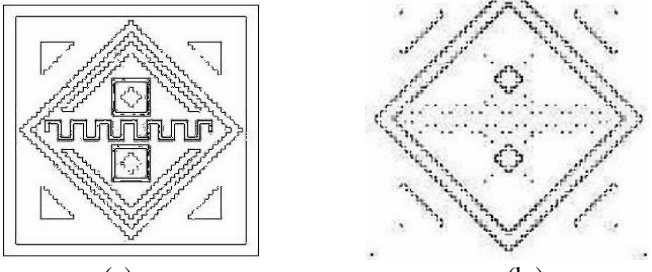

(a) (b)

Fig. 3. (a) sample pattern of the image (b) corner detection of the sample pattern of the image

2.2 Lines Detection

On every move of the 3X3 window, the RT of each boundary values sequence is checked for the following conditions: (a) the number of RT elements that are less than T must be 4. (b) The first four RT elements including the CPI should be greater than T. In such a case, the central pixel has to be a midpoint of a line and so is chosen.

The overall effect is that the resulting image would consist only of straight lines.

2.3 Curves Detection

A curve is not a straight line. Hence, the algorithm for detecting curves advocates the invalidity of the conditions for detecting lines.

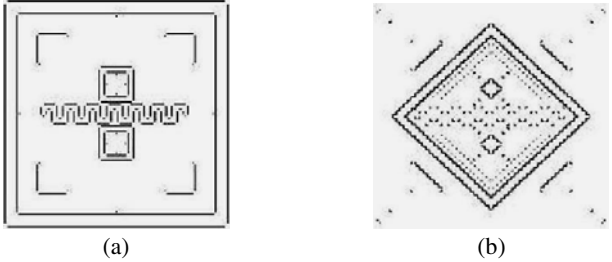

(a) (b)

Fig. 4. (a) Lines detected from the sample pattern of the image (b) Corners detected from the sample pattern of the image

2.4 Dot Detection

Dots are isolated points. If most of the RT elements are below the average value then the central pixel value is treated as an isolated point.

3 Textures Classification

The term 'texture' refers to 'repeated patterns' in an image [17], [18]. Many applications do require detection of textures in a given image [19], [20]. One can choose four different algorithms Rank1, Rank2, Rank3 and Rank4to detect textures present in an image in four different directions like North-South, East-West, North West-South East and North East-South West.

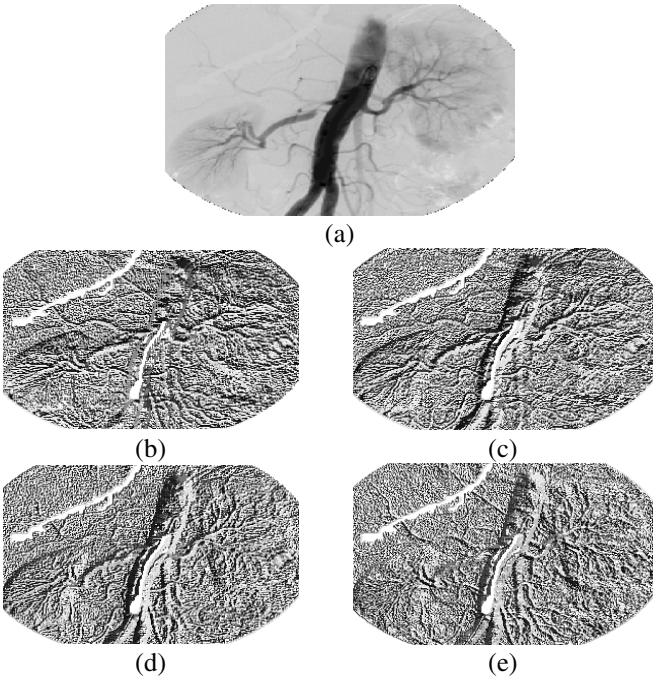

Fig. 5. (a) Example image (b) Rank 1 texturized image (c) Rank 2 texturized image (d) Rank 3 texturized image (e) Rank 4 texturized image

The given image is scanned by a 3X3 window. Each of the image values x(0), x(1), x(2), x(3), x(4), x(5), x(6), x(7)is compared with the central image pixel value. If x(i) : $0 \leq i \leq 7$ is less than or equal to the central pixel value, then x(i) is replaced by 0, otherwise by a 1. This yields a binary word of length 8. The decimal equivalent of this word is stored as the central image pixel value. The entire image is scanned in this manner and thus the resulting image would turn out to be the textured image.

The algorithm for texturizing an image remains same for all four cases with the exception that Rank 1 algorithm uses the sequence x(0), x(1), x(2), x(3), x(4), x(5), x(6), x(7);Rank 2 algorithm uses the sequence x(1), x(2), x(3), x(4), x(5), x(6), x(7), x(0) ; Rank 3 algorithm uses the sequence x(2), x(3), x(4), x(5), x(6), x(7), x(0), x(1) and Rank 4 algorithm uses the sequence x(3), x(4), x(5), x(6), x(7), x(0), x(1), x(2). The original ultra scanned image of a human artery and all the four textured versions of the image using Rank1, Rank2, Rank3 and Rank4 algorithms are given in the right column. Textures in a specific orientation need not be the same as those in another orientation. Refer to the images shown in Fig.5 to verify this fact.

Now the Rajan Transform is used to de detect various features of textures. The various features such as corners, curves, dots and lines are detected and their negative images are shown in Fig.6, Fig 7 , Fig 8 and Fig.9.

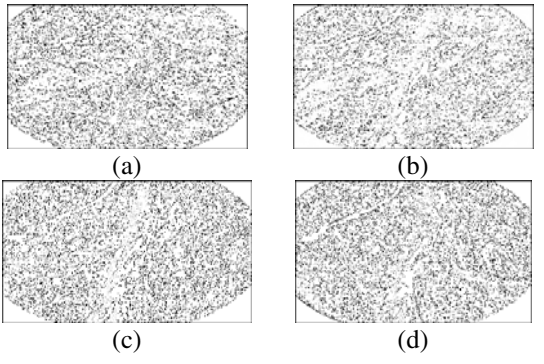

Fig. 6. (a) Detected corner feature of the texture using rank1 filter (b) Detected corner feature of the texture using rank2 filter (c) Detected corner feature of the texture using rank3 filter (b) Detected corner feature of the texture using rank4 filter

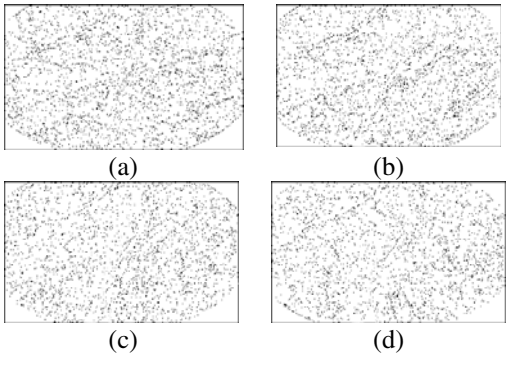

Fig. 7. (a)Detected curve feature of the texture using rank1 filter (b) Detected curve feature of the texture using rank2 filter :(a)Detected curve feature of the texture using rank3 filter (b) Detected curve feature of the texture using rank4 filter

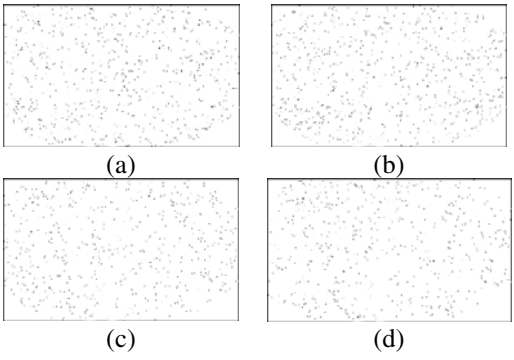

Fig. 8. (a)Detected dot feature of the texture using rank1 filter (b) Detected dot feature of the texture using rank2 filter :(a)Detected dot feature of the texture using rank3 filter (b) Detected curve feature of the texture using rank4 filter

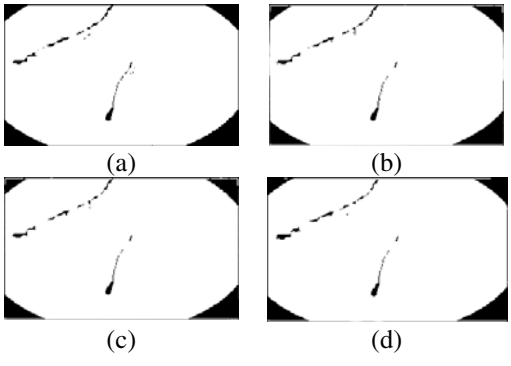

Fig. 9. (a)Detected line feature of the texture using rank1 filter (b) Detected line feature of the texture using rank2 filter :(a)Detected line feature of the texture using rank3 filter (b) Detected line feature of the texture using rank4 filter

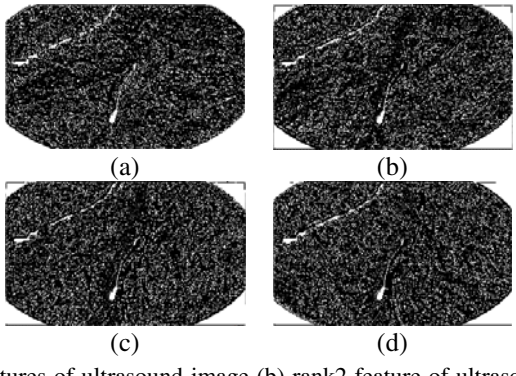

Fig.10. (a) rank1 features of ultrasound image (b) rank2 feature of ultrasound image (c) rank3 features of ultrasound image (d) rank4 features of ultrasound image

All the features superimposed to yield what we call as feature images. In what follows, we provide the feature images of the example ultrasound image used in this paper.

Low pass filtering is carried out on all the feature images of the example which reduces the entropy of the images to obtain the Fig11.

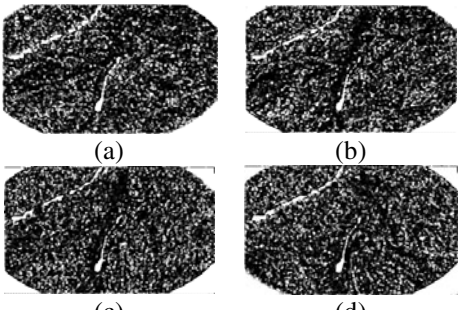

Fig. 11. (a) rank1 features of ultrasound image after low pass filtering (b)rank2 feature of ultrasound image after low pass filtering (c)rank3 features of ultrasound image after low pass filtering (d)rank4 features of ultrasound image after low pass filtering

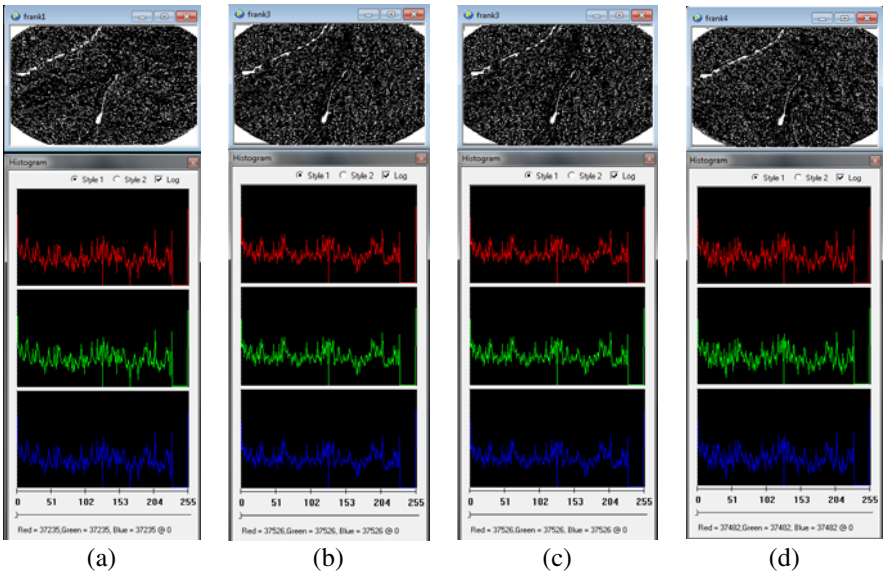

Fig. 12. (a) Histogram of rank1 feature image (b) Histogram of rank2 feature image (c) Histogram of rank3 feature image (d)Histogram of rank4 feature image

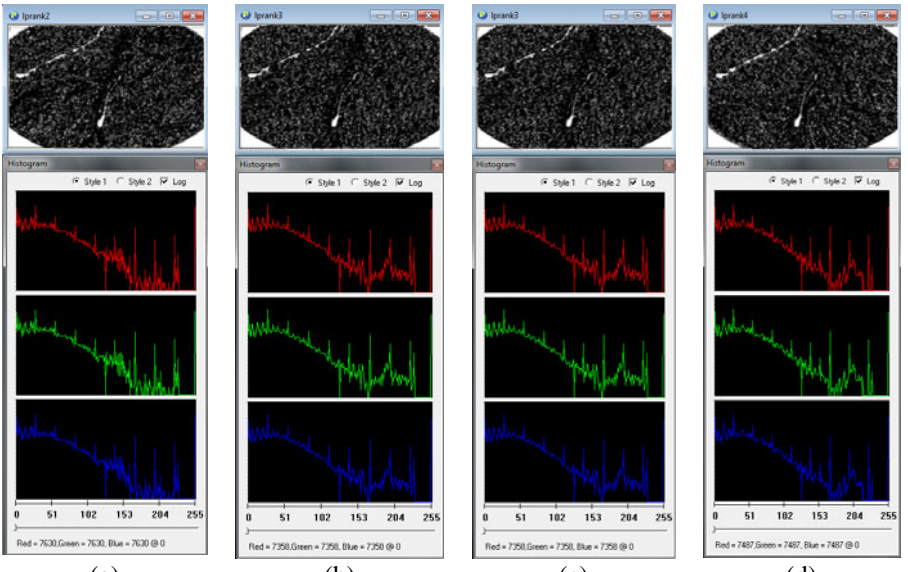

(a) (b) (c) (d)

Fig. 13. (a) Histogram of rank1 low pass filtered feature image (b) Histogram of rank2 low pass filtered feature image (c) Histogram of rank3 low pass filtered feature image (d) Histogram of rank4 low pass filtered feature image.

4 Experimental Setup and Results

The image which is shown in the above example has been used as a test image. Logical image processing system Software 3.0 is used for analysis. A desktop PC with 280GB and 4GB RAM was used to process the images. All the features have dots ,curves , corners and lines have been independently detected using RT based pattern recognition algorithms. The corresponding histograms have also been evaluated for visualize the image which is hidden in the original image.

5 Related Work

Texture analysis has played a prominent role to solve tissue characterization problems in medical imaging [21].Several researchers have been working to develop methods to obtain the tissue characterization of the ultrasound image and in this context many methods have been developed. In [22] ,the authors evolved a technique for reducing the noise of the image in order to have a clear representation of the tissue. The noise reduction is achieved by verging sets of images when the least variance in diameter of the image occurs. At the end, a fuzzy logic based expert system has been used to discriminate the tissues. In [23] .the authors proposed the use of co-occurrence matrices texture analysis and fractal texture analysis to characterize tissues. Thirteen features plus fractal dimension derived from Brownian motion were

used for this purpose. In [24], use co-occurrence matrices and discriminate analysis were used to evaluate different kind of tissues in the ultrasound images.

Further work has been done with the idea of using texture feature extractors for processing the ultrasound images, though not specifically centered on tissue characterization . In [25] , so many methods derivatives of Gaussian, wavelets, co-occurrence matrices, Gabor filters have been used for finding local moments so as to discriminate blood. This last line of investigation overcomes one of the most significant drawbacks of the texture based tissue characterization systems, the speed. Hence we proposed a novel method for tissue characterization, which uses the pattern recognition capabilities of the Rajan Transform.

6 Conclusions

In this paper, we have proposed a novel technique for tissue characterization in ultrasound images. This paper uses Spectral characterization of Rank Filters Based Directional Textures of Digital Images Using Rajan Transform, this transform is homomorphic transform and hence it can be to used to classify various features of an image. Texture is a spatially repeated pattern. So , this transform is very much useful for tissue characterization and thus clinicians would benefit to great extend in the form of diagnostic tool analysis the image and hence to diagnose the problem. The present method can also perform effective feature extraction, and also characterize the tissues of images precisely. Future work rests on the application of the present method to different kinds of medical images for classification purposes.

Acknowledgments. The authors sincerely thank the administration of Pentagram Research Centre Pvt Limited, Hyderabad, India for the permitting us to use their software Logical Image Processing System and for the unparallel support extended to the authors in developing the technology introduced in this paper. We also thank Dr. E.G Rajan for his invaluable suggestions and feedback while preparing the contents of this paper.

References

1. Hill, C.R., Bamber, J.C., Ter haar, G.R.: Physical principles of medical Ultrasonics, 2nd edn. John Wiley, Chichester (2004)
2. Saniie, J., Nagle, D.T.: Pattern recognition in the ultrasonic imaging of reverberant multilayered structures. IEEE Trans. Ultrasound, Ferroelectric, Frequency Contr. 36, 80–92 (1989)
3. Fenster, A., Surry, K., Smith, W., Gill, J., Downey, D.: 3D ultrasound imaging: applications in image-guided therapy and biopsy. Computer Graphics, 557–568 (2002)
4. Schmitz, G., Ermert, H., Senge, T.: Tissue-characterization of the prostate using radio frequency ultrasonic signals. IEEE Transactions on Ultrasound Ferroelectrics & Frequency Control 46(1), 126–138 (1999)
5. Materka, A., Strzelecki, M.: Texture Analysis Methods – A Review, A Review, Technical University of Lodz, Institute of Electronics, COST B11 report, Brussels (1998)

6. Grigorescu, S.E., Petkov, N., Kruizinga, P.: Comparison of Texture Features Based on Gabor Filters. IEEE Transactions on Image Processing 11(10), 1160–1167 (2002)
7. Noble, J.A.: Ultrasound image segmentation and tissue characterization. Part H: J. Engineering in Medicine 223, 1–10 (2009)
8. Noble, J., Boukerroui, D.: Ultrasound image segmentation: a survey. IEEE Transaction in Med. Imaging 25(8), 987–1010 (2006)
9. Yang, C., Zhu, H., Wu, S., Bai, Y., Gao, H.: Correlations Between B-Mode Ultrasonic Image Texture Features and Tissue temperature in Microwave Ablation by the American Institute of Ultrasound in Medicine. J. Ultrasound Medicine, 1787–1799 (2010)
10. Prager, R.W., Gee, A.H., Treece, G.M., Kingsbury, N.G., Lindop, J.E., Gomersall, H., Shin, H.-C.: Deconvolution and Elastography based on three-dimensional ultrasound. In: Proceedings of the IEEE International Ultrasonics Symposium (IUS 2008), Beijing, People's republic of China, November 2-5, pp. 548–557 (2008)
11. Fenster, A., Surry, K., Smith, W., Gill, J., Downey, D.: 3D Ultrasound imaging: applications in image guided therapy and biopsy. Computer Graphics, 557–568 (2002)
12. Fitzpatrick, J.M., Reinhardt, J.M.: Prostate ultrasound image segmentation using level set-based region flow with shape guidance. SPIE (2005)
13. Kubota, R., Kunihiro, M., Suetake, N., Uchino, E., Hashimoto, G., Hiro, T., Matsuzaki, M.: An Intravascular Ultrasound-based Tissue Characterization Using Shift-invariant Features Extracted by Adaptive Subspace SOM. International Journal of Biology and Biomedical Engineering (2008)
14. Rajan, E.G.: Symbolic Computing - Signal and image processing. Anshan Publications, Kent (2003)
15. Mandalapu, E.N., Rajan, E.G.: Rajan Transform and its Uses in Pattern Recognition. Informatica 33, 213–220 (2009)
16. Mandalapu, E.N., Rajan, E.G.: Two Dimensional Object Recognition Using Rajan Transform. Engineering Letters 13, 3, EL_13_3_7 Advance online publication (2006)
17. Randen, T.R., Husoy, J.H.: Filtering for texture classification: a comparative study. IEEE Trans. Pattern Anal. Machine Intelligent 21, 291–310 (1999)
18. Noble, J.A.: Ultrasound image segmentation and tissue characterization. Journal of Engineering in Medicine (2010)
19. Landini, L., Verrazzani, L.: Spectral characterization of tissues microstructure by ultrasounds: a stochastic approach. IEEE Transactions Ultrasonics, Ferroelectrics and Frequency Control (1990)
20. Lizzi, F.L., Feleppa, E.J., Kaisar Alam, S., Deng, C.X.: Ultrasonic spectrum analysis for tissue evaluation. Pattern Recognition Letters (2003)
21. Hill, C.R., Bamber, J.C., ter Haar, G.R.: Physical principles of medical ultrasonics, 2nd edn. (2004)
22. Vandenberg, J.: Arterial imaging techniques and tissue characterization using fuzzylogic. In: Proceedings of the 1994 Second Australian and New Zealand Conference on Intelligent Information Systems, 239–243 (1994)
23. Nailon, W., McLaughlin, S.: Intravascular ultrasound image interpretation. In: Proceeding Of the International Conference on Pattern Recognition. IEEE Computer Society, Austria (1997)
24. Dixon, K.: Characterization of coronary plaque in intravascular ultrasound histological Correlation. In: IEEE Conference (1997)
25. Pujol, O., Radeva, P.: Automatic segmentation of lumen in intravascular ultrasound images: An evaluation of texture feature extractors. In: Proceedings for IBERAMIA (2002)